

Prompt cusps in hierarchical dark matter halos: Implications for annihilation boost

Shin'ichiro Ando,^{a,b} Martín Moró^{a,c} and Youyou Li^a

^aGRAPPA Institute, University of Amsterdam, Science Park, 1098 XH Amsterdam, The Netherlands

^bKavli Institute for the Physics and Mathematics of the Universe, University of Tokyo, Chiba 277-8583, Japan

^cCentro de Investigaciones Energéticas, Medioambientales y Tecnológicas (CIEMAT), E-28040 Madrid, Spain

E-mail: s.ando@uva.nl

Abstract. Recent simulations have identified long-lived “prompt cusps”—compact remnants of early density peaks with inner profiles $\rho \propto r^{-3/2}$. They can survive hierarchical assembly and potentially enhance signals of dark matter annihilation. In this work, we incorporate prompt cusps into the semi-analytic substructure framework SASHIMI, enabling a fully hierarchical, environment-dependent calculation of the annihilation luminosity that consistently tracks subhalos, sub-subhalos, and tidal stripping. We assign prompt cusps to first-generation microhalos and propagate their survival through the merger history, including an explicit treatment of cusps associated with stripped substructure. We find that the substructure hierarchy converges rapidly once a few levels are included, and that prompt cusps can raise the total annihilation boost of Milky-Way-size hosts at $z = 0$ to $B \sim \mathcal{O}(10)$ for fiducial cusp-occupation assumptions, compared to a subhalo-only baseline of $B_{\text{sh}} \sim \text{few}$. Across a wide range of host masses and redshifts, prompt cusps increase the normalization of $B(M_{\text{host}}, z)$ while largely preserving its mass and redshift trends. Compared to universal-average, peak-based estimates, our fiducial boosts are lower by about an order of magnitude, primarily reflecting a correspondingly smaller inferred cusp abundance in host halos, highlighting the importance of unifying peak-based cusp formation with merger-tree evolution and environmental dependence.

Contents

1	Introduction	1
2	Prompt cusps	3
2.1	Formation of cusps from primordial density peaks	3
2.2	Collapse time and characteristic radii	4
2.3	Annihilation luminosity of a prompt cusp	5
2.4	Prompt cusp properties and annihilation enhancement	5
3	Semi-analytical treatment of halo substructure and prompt cusps	6
3.1	SASHIMI: weighted subhalo catalog	6
3.2	Hierarchical substructure and effective prompt-cusp counts	7
3.3	Tidal stripping of hierarchical substructure and cusp survival	8
4	Results	9
5	Discussion	12
5.1	Comparison with earlier work	12
5.2	Possible origin of the cusp-abundance difference	12
5.3	Future directions	13
6	Conclusions	14

1 Introduction

Cosmological observations across a wide range of scales indicate that more than 80% of the matter content of the Universe is in the form of non-luminous, non-baryonic dark matter. Despite this strong empirical support (from the cosmic microwave background, large-scale structure, and gravitational lensing), the microscopic nature of dark matter remains unknown. In the standard cold dark matter (CDM) paradigm, dark matter is assumed to be non-relativistic during structure formation, leading naturally to hierarchical clustering: the smallest bound objects collapse first and subsequently merge to form larger halos. If dark matter consists of weakly interacting massive particles (WIMPs), such as the supersymmetric neutralino, the earliest gravitationally bound halos can be extremely small, with masses as low as $M \sim 10^{-6} M_{\odot}$ and extending up to cluster scales of $M \sim 10^{15} M_{\odot}$ [1–6]. As these small halos form at high redshift and merge into larger hosts, many are tidally disrupted while others survive as long-lived bound remnants—commonly referred to as subhalos—embedded within the larger structures that comprise the cosmic web.

The abundance of substructure within CDM halos has important observational implications. Self-bound subhalos significantly enhance the annihilation rate of WIMP dark matter, boosting the resulting gamma-ray luminosity compared to that of a smooth host halo. This enhancement has motivated extensive studies on the detectability of annihilation signals and the role of substructure in shaping the diffuse gamma-ray background [7–19]. A key ingredient in such predictions is the assumed inner density profile of halos and subhalos.

Numerical simulations have long indicated that CDM halos follow a nearly universal density profile, commonly parametrized by the Navarro-Frenk-White (NFW) form, $\rho(r) \propto$

r^{-1} in the inner regions and $\rho(r) \propto r^{-3}$ at large radii [20]. However, recent high-resolution simulations have revealed a qualitatively different behavior in the earliest-forming halos. Small-scale peaks in the initial density field can undergo rapid, nearly self-similar collapse, producing extremely steep inner cusps with $\rho(r) \propto r^{-1.5}$ —significantly steeper than the NFW profile [21–26]. These prompt cusps appear generically in the first generation of halos, with their number and properties determined by the statistics of primordial density peaks. Only peaks with sufficiently low ellipticity and without strong interactions with neighboring structures form such cusps; others relax to an NFW-like structure instead. Importantly, simulations suggest that once formed, prompt cusps tend to survive subsequent mergers and accretion events, remaining as long-lived features embedded in the inner regions of larger halos [24].

The existence of prompt cusps has significant implications for indirect searches for dark matter. Because the annihilation rate scales with the square of the local dark matter density, the extremely steep $r^{-1.5}$ profiles generated by the rapid collapse of small-scale peaks can substantially enhance the gamma-ray emissivity associated with WIMP annihilation. Delos and White [26] demonstrated that, for thermally produced WIMPs, every solar mass of dark matter may contain thousands of Earth-mass prompt cusps, leading to an overall annihilation rate that exceeds predictions based on smooth-halo or traditional subhalo models by at least an order of magnitude. Their analysis further showed that prompt-cusp emission is less centrally concentrated than the conventional NFW-based expectation, thereby modifying the relative importance of diffuse components such as the extragalactic gamma-ray background [26]. Subsequent works test these predictions against observations. Constraints from the isotropic gamma-ray background measured by the *Fermi*-LAT have been shown to strongly limit the viable parameter space for WIMP annihilation once prompt cusps are included [25]. Additional studies have considered environmental effects such as disruption by stars and tidal fields, finding that cusp survival can significantly influence the expected annihilation signal [27]. Observations of galaxy clusters have been used to place further constraints on prompt-cusp annihilation scenarios, in some cases suggesting substantial tension between cusp-enhanced predictions and current gamma-ray limits [28].

Importantly, nearly all existing analyses characterize the contribution of prompt cusps using a *universal average* boost factor; they assume that cusp properties and survival statistics are identical across cosmic environments. While this approach provides a valuable first estimate, it cannot capture the potential dependence of annihilation enhancement on host-halo mass, redshift, merger history, or the hierarchical structure of subhalos and their internal evolution. To address these shortcomings, in this work we incorporate prompt-cusp physics directly into the semi-analytic substructure framework SASHIMI [17],¹ enabling a fully hierarchical and environment-dependent treatment of annihilation signals. (For SASHIMI for other non-cold dark matter candidates, see, e.g., Refs. [29, 30].) Specifically, we embed one prompt cusp into every first-generation subhalo generated by SASHIMI, and we track its survival within the full hierarchy of substructures, including sub-subhalos and even smaller progenitors. Cusp disruption is modeled through a parameterization that captures the tidal evolution of each host–subhalo system, allowing us to propagate survival probabilities consistently across the merger history. With this enhanced model, we re-evaluate the annihilation boost factor for a wide range of host-halo masses and find that Milky-Way–like halos generically exhibit total boosts of order tens—comparable to those inferred

¹<https://github.com/shinichiroando/sashimi-c>

in previous universal-average studies [26], but now obtained through a physically grounded, self-consistent hierarchical calculation. We also release an updated version of the public SASHIMI package, which includes our prompt-cusp implementation and associated tools for annihilation boost calculations.

The remainder of this paper is organized as follows. In Sec. 2, we summarize the formation of prompt cusps and the physical quantities that characterize them. Section 3 reviews the SASHIMI framework and describes how we model the hierarchical population of subhalos and sub-subhalos, by embedding prompt cusps. In Secs. 4, we present the evolution and survival of prompt cusps within host halos and incorporate their contribution into the annihilation signal by embedding one cusp into each first-generation subhalo. We then evaluate the resulting annihilation boost across host-halo masses and compare our findings with previous studies. Finally, Sec. 5 summarizes our conclusions and discusses prospects for future work.

2 Prompt cusps

The theoretical framework adopted in this work follows the analysis of Refs. [24, 26, 31], which showed that small-scale peaks in the primordial density field undergo rapid, nearly self-similar collapse and form extremely steep density cusps. These structures arise at the earliest epochs of hierarchical structure formation, prior to virialization into the familiar NFW profile, and retain a characteristic inner slope $\rho \propto r^{-1.5}$ that persists unless disrupted by subsequent mergers or encounters. In this section, we summarize the essential physics governing the formation of prompt cusps, their characteristic scales, and the resulting annihilation luminosity.

2.1 Formation of cusps from primordial density peaks

Density fluctuations in the early universe are described by the matter power spectrum $P(k)$, which can be written as $P(k) \propto k^{n_s} T^2(k)$, where $n_s \approx 0.965$ is the power-law index of the primordial curvature perturbation [32] and $T(k)$ is the transfer function encoding the suppression of small-scale modes and the growth of perturbations prior to matter–radiation equality [33, 34]. The dimensionless form of the spectrum is $\mathcal{P}(k) = k^3 P(k)/(2\pi^2)$, and its time evolution is governed by the linear growth factor $D(z)$: $\mathcal{P}(k, z) = D^2(z) \mathcal{P}(k)|_{z=0}$. For a thermal WIMP with mass $m_\chi = 100$ GeV and kinetic decoupling temperature $T_{\text{kd}} = 30$ MeV, small-scale power is suppressed below the free-streaming scale of $k_{\text{fs}} = 1.06 \times 10^6 \text{ Mpc}^{-1}$ [35], by multiplying $\mathcal{P}(k, z)$ further by $\exp(-k^2/k_{\text{fs}}^2)$.

Peaks in the primordial density field, $\delta(\mathbf{r}) = (\rho - \bar{\rho})/\bar{\rho}$, collapse first along their steepest directions. For sufficiently low ellipticity, the collapse proceeds in a nearly radial fashion and produces a self-similar density profile,

$$\rho(r) = A r^{-3/2}, \quad (2.1)$$

where the amplitude A depends on the peak height and curvature. Delos and White [24, 26] showed that

$$A \simeq 24 \bar{\rho}_0 a_{\text{coll}}^{-3/2} R^{3/2}, \quad (2.2)$$

with $\bar{\rho}_0$ the present-day mean dark matter density and R the characteristic comoving curvature scale, $R = |\delta/\nabla^2\delta|^{1/2}$, where δ and $\nabla^2\delta$ are the linearly extrapolated density contrast and curvature at the peak position.

To characterize peaks in the Gaussian density field with δ and $\nabla^2\delta$, we define the spectral moments as

$$\sigma_j^2 = \int_0^\infty \frac{dk}{k} k^{2j} \mathcal{P}(k), \quad j = 0, 1, 2, \quad (2.3)$$

which fully determine the statistics of peaks. Following Ref. [33], the joint distribution of peak height and curvature is parametrized by $\nu \equiv \delta/\sigma_0$ and $x \equiv -\nabla^2\delta/\sigma_2$. We draw ν and x from the peak distribution (see, e.g., Appendix A of Ref. [26]), reconstructing the physical peak quantities via $\delta = \nu\sigma_0$, $\nabla^2\delta = -x\sigma_2$, to calculate the characteristic comoving scale of the peak $R = |\delta/\nabla^2\delta|^{1/2}$.

2.2 Collapse time and characteristic radii

The collapse scale factor for a peak of height $\delta(a)$ at scale factor a is [26]

$$a_{\text{coll}} = \left[f_{\text{ec}}(e, p) \frac{\delta_c}{\delta(a)} \right]^{1/g} a, \quad (2.4)$$

where $f_{\text{ec}}(e, p)$ is the ellipsoidal-collapse correction sampled from a distribution given the peak height δ [36], $\delta_c = 1.686$ is the critical threshold for spherical collapse, and $g \simeq 0.901$ is the small-scale growth index. In order for a cusp to form in each peak, the ellipticity e and prolateness p need to satisfy the condition: $e^2 - p|p| < 0.26$. A fraction f_{coll} of all the peaks will collapse to form a cusps in them.

Once formed, the cusp extends out to a physical radius $r_{\text{cusp}} \simeq 0.11 a_{\text{coll}} R$. The inner boundary is set by the primordial maximum coarse-grained phase-space density [37], which defines the core radius $r_{\text{core}} \simeq [3 \times 10^{-5} G^{-3} f_{\text{max}}^{-2} A^{-1}]^{2/9}$, where the maximum phase-space density for a thermal relic is

$$f_{\text{max}} = \frac{1}{(2\pi)^{3/2}} \left(\frac{m_\chi}{T_{\text{kd}}} \right)^{3/2} \bar{\rho}_0 a_{\text{kd}}^{-3}. \quad (2.5)$$

Because Liouville's theorem guarantees that the coarse-grained phase-space density of collisionless dark matter can never exceed its initial value [37], the self-similar $\rho(r) = Ar^{-3/2}$ profile must eventually flatten at sufficiently small radii. This defines the physical core radius r_{core} , inside which the implied phase-space density of the cusp would otherwise exceed f_{max} . It is therefore useful to introduce the corresponding core density,

$$\rho_{\text{core}} \equiv \rho(r_{\text{core}}) = A r_{\text{core}}^{-3/2}, \quad (2.6)$$

which marks the innermost region where the cusp is regulated by the primordial phase-space bound. The value of r_{core} is obtained by equating f_{max} with the phase-space density implied by the power-law cusp, yielding

$$r_{\text{core}} \simeq [3 \times 10^{-5} G^{-3} f_{\text{max}}^{-2} A^{-1}]^{2/9}. \quad (2.7)$$

This core radius plays a central role in determining the annihilation luminosity of a prompt cusp, since the integral of ρ^2 is dominated by the region between r_{core} and r_{cusp} .

2.3 Annihilation luminosity of a prompt cusp

Because the annihilation rate scales as ρ^2 , prompt cusps are exceptionally bright sources compared to NFW-like inner profiles. Integrating the density-squared profile between r_{core} and r_{cusp} gives the annihilation “luminosity parameter” [27]

$$J_{\text{cusp}} = \int_{r_{\text{core}}}^{r_{\text{cusp}}} 4\pi r^2 \rho^2(r) dr = 4\pi A^2 \left[0.531 + \ln\left(\frac{r_{\text{cusp}}}{r_{\text{core}}}\right) \right].$$

The quantity J_{cusp} appears repeatedly throughout this work and forms the basic unit of annihilation luminosity for each prompt cusp before any tidal evolution or survival probability is applied.

2.4 Prompt cusp properties and annihilation enhancement

The properties of individual prompt cusps are determined by a small set of peak parameters, namely the peak height ν , curvature x , and the ellipticity–prolateness parameters (e, p) . These quantities are sampled from their joint probability distributions as prescribed by peak statistics [33]. All remaining cusp properties then follow deterministically from (ν, x, e, p) through the collapse condition and subsequent dynamical relations.

Using this sampling procedure, we compute ensemble-averaged properties of prompt dark matter cusps. Averaging over the population of collapsing peaks, we obtain the following representative values:

$$\langle R \rangle \simeq 1.5 \text{ pc}, \tag{2.8}$$

$$\langle a_{\text{coll}} \rangle \simeq 0.09, \tag{2.9}$$

$$\langle A \rangle \simeq 1.5 \times 10^{-4} M_{\odot} \text{ pc}^{-1.5}, \tag{2.10}$$

$$\langle r_{\text{core}} \rangle \simeq 1.9 \times 10^{-5} \text{ pc}, \tag{2.11}$$

$$\langle r_{\text{cusp}} \rangle \simeq 1.2 \times 10^{-2} \text{ pc}, \tag{2.12}$$

$$\langle M_{\text{cusp}} \rangle \simeq 9 \times 10^{-7} M_{\odot}, \tag{2.13}$$

$$f_{\text{coll}} \simeq 0.48, \tag{2.14}$$

which are in good agreement with those obtained by Ref. [26].

The characteristic curvature scale R and the collapse scale factor a_{coll} indicate that prompt cusps form at very early epochs, well before nonlinear structure formation on galactic scales. Roughly half of the peaks that satisfy the collapse condition proceed to form cusps, with a fraction $f_{\text{coll}} \simeq 0.48$. The resulting cusps are highly compact objects with a steep inner density profile, characterized by a small core radius $r_{\text{core}} \ll r_{\text{cusp}}$. The normalization parameter A sets the amplitude of the density profile [Eq. (2.1)], which leads to a total cusp mass well below stellar scales, $M_{\text{cusp}} \sim 10^{-6} M_{\odot}$. Despite their small mass, the extremely high central densities result in a significant enhancement of the dark matter annihilation signal. The mean annihilation factor per cusp is found to be

$$\langle J_{\text{cusp}} \rangle \simeq 4.7 \times 10^{-6} M_{\odot}^2 \text{ pc}^{-3}, \tag{2.15}$$

demonstrating that prompt cusps can provide a non-negligible contribution to annihilation observables once their abundance is taken into account.

3 Semi-analytical treatment of halo substructure and prompt cusps

3.1 SASHIMI: weighted subhalo catalog

To model the contribution of substructure to dark matter annihilation signals, we employ the Semi-Analytical SubHalo Inference ModelIng (SASHIMI; [17, 18]). SASHIMI provides an analytic realization of a subhalo population within a host halo by sampling the subhalo mass-accretion history and its subsequent tidal evolution. Rather than generating individual halos in an N -body sense, the method constructs a weighted catalog of subhalos whose ensemble averages reproduce the underlying distribution functions. In this work, we compute the rms overdensity $\sigma(M)$ from a linear matter power spectrum that includes a small-scale free-streaming suppression, $P(k) \rightarrow P(k) \exp(-k^2/k_{\text{fs}}^2)$. Following common practice for suppressed-small-scale-power scenarios, we evaluate $\sigma(M)$ using a k -space top-hat (sharp- k) filter, with an upper cutoff $k_{\text{max}} = \alpha/R$ (where R is the Lagrangian radius associated with mass M), which is known to provide a robust mapping between the cutoff scale and the halo mass function in excursion-set calculations [38]. The parameter α encodes the residual ambiguity of this mapping; we fix it to $\alpha = 1.8$ by matching $\sigma(M)$ to the real-space top-hat result in the large-mass regime. The resulting $\sigma(M)$ is then used consistently in the extended-Press-Schechter (EPS)-based ingredients of SASHIMI.

Each subhalo in the catalog, labeled by an index i , is assigned a set of structural parameters $(\rho_{s,i}, r_{s,i}, r_{t,i})$, where $\rho_{s,i}$ and $r_{s,i}$ are the characteristic density and scale radius of an NFW profile, and $r_{t,i}$ is the truncation radius induced by tidal stripping. In addition, each entry carries a weight factor w_i , which represents the number of physical subhalos corresponding to that realization. As a result, integrals over the distribution of subhalo properties, can be evaluated as weighted sums over the catalog,

$$\int d\boldsymbol{\theta} \frac{dN_{\text{sh}}}{d\boldsymbol{\theta}} (\dots) \longrightarrow \sum_i w_i (\dots)_i. \quad (3.1)$$

where $\boldsymbol{\theta} = (\rho_s, r_s, r_t, \dots)$ represents the subhalos' density profile parameters among others, and $dN_{\text{sh}}/\boldsymbol{\theta}$ is their joint distribution function.

For example, the annihilation luminosity parameter of an individual subhalo i is given by

$$J_{\text{sh},i} = \int_0^{r_{t,i}} dr 4\pi r^2 \rho_{\text{sh}}^2(r | \rho_{s,i}, r_{s,i}, r_{t,i}) = \frac{4\pi}{3} \rho_{s,i}^2 r_{s,i}^3 \left[1 - \frac{1}{(1 + r_{t,i}/r_{s,i})^3} \right], \quad (3.2)$$

where $\rho_{\text{sh}}(r)$ denotes the truncated NFW profile. In the baseline SASHIMI implementation, the above expression describes the annihilation luminosity of a single (resolved) subhalo realization. Additional enhancement from unresolved substructure *within* subhalos (i.e., sub-subhalos and higher-order levels) can be incorporated in a recursive manner; we refer the reader to Refs. [17, 18] for a detailed treatment and its impact on the boost factor. In this work, we will revisit the hierarchical contribution explicitly in the next subsection, where we quantify the effective subhalo counts when including sub n -subhalos. The total contribution from all subhalos in a host halo can then be written as

$$J_{\text{sh, total}} = \int d\rho_s \int dr_s \int dr_t \frac{d^3 N_{\text{sh}}}{d\rho_s dr_s dr_t} J_{\text{sh}}(\rho_s, r_s, r_t) \simeq \sum_i w_i J_{\text{sh},i}. \quad (3.3)$$

Using this framework, Refs. [17, 18] demonstrated that the annihilation boost factor due to subhalos in a Milky-Way-size halo is modest, typically $B_{\text{sh}} \sim 2\text{--}3$. In the following,

Table 1. Effective number of subhalos in a Milky-Way-size host ($M = 10^{12} M_\odot$, $z = 0$) when including hierarchical substructure up to sub n -subhalos. We additionally report the split into subhalos inside the truncation radius of their immediate parent, $N_{\text{sh,in}}^{(n)}$, and those in the stripped region, $N_{\text{sh,stripped}}^{(n)}$.

n	$N_{\text{sh}}^{(n)}$	$N_{\text{sh,in}}^{(n)}$	$N_{\text{sh,stripped}}^{(n)}$
0	2.7×10^{15}	2.7×10^{15}	0
1	6.6×10^{15}	3.3×10^{15}	3.3×10^{15}
2	9.2×10^{15}	3.3×10^{15}	5.9×10^{15}
3	1.03×10^{16}	3.3×10^{15}	7.0×10^{15}
4	1.06×10^{16}	3.3×10^{15}	7.3×10^{15}

we extend this formalism by embedding prompt cusps within each subhalo realization and reassessing the resulting annihilation enhancement.

3.2 Hierarchical substructure and effective prompt-cusp counts

As a concrete example, we consider a Milky-Way-size host halo with $M = 10^{12} M_\odot$ at $z = 0$. We include the hierarchy of substructure up to sub n -subhalos.

At zeroth order ($n = 0$), only subhalos are present and each subhalo's density profile is assumed to be smooth. The expected number of subhalos can be written as the sum of weights in the SASHIMI catalog,

$$N_{\text{sh}}^{(0)}(M, z) = \sum_i w_i(M, z), \quad (3.4)$$

which evaluates to 2.7×10^{15} . Next, at first order ($n = 1$), we include sub-subhalos within each host-level subhalo. The effective number of subhalos is then given by

$$N_{\text{sh}}^{(1)}(M, z) = \sum_i w_i(M, z) \left[1 + \sum_j w_j(m_{a,i}, z_{a,i}) \right], \quad (3.5)$$

where $m_{a,i}$ and $z_{a,i}$ are the accretion mass and accretion redshift of the i th subhalo, and the inner sum runs over the sub-subhalo catalog conditioned on $(m_{a,i}, z_{a,i})$.

Proceeding in the same manner, including sub n -subhalos corresponds to iterating this construction. For example, up to $n = 3$, we write

$$N_{\text{sh}}^{(3)}(M, z) = \sum_i w_i(M, z) \left\{ 1 + \sum_j w_j(m_{a,i}, z_{a,i}) \left[1 + \sum_k w_k(m_{a,j}, z_{a,j}) \right. \right. \\ \left. \left. \times \left(1 + \sum_l w_l(m_{a,k}, z_{a,k}) \right) \right] \right\}. \quad (3.6)$$

We compute these effective counts up to $n = 4$ for $M = 10^{12} M_\odot$ at $z = 0$ and summarize the results in Table 1.

In hierarchical structure formation, dark matter (sub)halos can be associated, to a good approximation, with peaks of the underlying (filtered) Gaussian density field, so that each subhalo realization may be linked to a corresponding peak in the initial conditions [33, 39, 40]. Motivated by this peak-based picture, we assume that a prompt cusp can form around a peak

only if the peak collapses sufficiently early, and that only a fraction f_{coll} of peaks satisfies this collapse condition (as discussed in the previous subsection). Moreover, not all newly formed prompt cusps are expected to survive subsequent evolution: tidal processing and mergers can erase a non-negligible fraction of cusps, leading to an overall survival probability of $f_{\text{surv}} \simeq 0.4\text{--}0.6$, as suggested by cosmological considerations of cusp survival [26].

Combining these ingredients, we parametrize the fraction of subhalos that host a *surviving* prompt cusp as

$$f_{\text{cusp}} \equiv f_{\text{coll}} f_{\text{surv}}, \quad (3.7)$$

such that f_{cusp} may be directly compared to the effective cusp fraction adopted in Ref. [26]. For reference, our peak-collapse estimate gives $f_{\text{coll}} \simeq 0.48$, and together with $f_{\text{surv}} \simeq 0.4\text{--}0.6$ this suggests $f_{\text{cusp}} \sim 0.2\text{--}0.3$, making $f_{\text{cusp}} = 0.25$ a plausible benchmark value. In what follows, we therefore explore $f_{\text{cusp}} = \{1, 0.5, 0.25\}$ as representative choices spanning optimistic to conservative scenarios for cusp survival within the subhalo population.

3.3 Tidal stripping of hierarchical substructure and cusp survival

In SASHIMI, the bound remnant of a subhalo after tidal evolution inside its host is described by a truncated NFW profile, such that the density drops rapidly outside the truncation radius r_t . In this approximation, substructure initially residing at radii $r > r_t$ is interpreted as being stripped from the parent subhalo and incorporated into the host halo as debris.

When hierarchical substructure is included (i.e., sub ^{n} -subhalos), the same stripping criterion can be applied recursively. We assume that sub ^{n} -subhalos are spatially distributed within their immediate host, the sub ^{$n-1$} -subhalo, according to a cored number-density profile,

$$n_{\text{sh}}^{(n)}(r) \propto \left[r^2 + (r_s^{(n-1)})^2 \right]^{-3/2}, \quad (3.8)$$

where $r_s^{(n-1)}$ is the scale radius of the sub ^{$n-1$} -subhalo. With this prescription, for each $(n-1)$ -level subhalo, only the n -level subhalos located within its truncation radius $r_t^{(n-1)}$ are retained as bound members of that branch, while those initially at $r > r_t$ are classified as stripped. Because prompt cusps are associated with the internal substructure, this distinction matters when translating the hierarchical census of subhalos into a census of *surviving* cusps.

We therefore split the effective number of sub ^{n} -subhalos into two components, $N_{\text{sh,in}}^{(n)}$ (inside r_t of their immediate parent, hence retained as bound members of the hierarchy) and $N_{\text{sh,stripped}}^{(n)}$ (initially outside r_t , hence stripped). In our fiducial implementation, stripped subhalos are assumed to be disrupted and phase-mixed into the host component, so that their associated cusps do not contribute as identifiable substructures. To allow for the possibility that a fraction of cusps in stripped material could remain self-bound and survive as compact remnants, we introduce an additional survival parameter $f_{\text{surv,stripped}}$, defined as the fraction of prompt cusps associated with stripped subhalos that persist after stripping. This ingredient is complementary to existing treatments that focus on the tidal stripping of the *cusps themselves* and on cusp disruption/merging criteria. For example, Ref. [26] explicitly models tidal stripping of prompt cusps and discuss cusp survival relative to subhalo disruption, but do not track the fate of a hierarchical sub-subhalo population split by a truncation radius within a semi-analytic subhalo catalog.

For a Milky-Way-size host ($M = 10^{12} M_{\odot}$, $z = 0$), the resulting effective subhalo counts are summarized in Table 1. The number of surviving cusps are then obtained by

$$N_{\text{cusp}} = f_{\text{cusp}} (N_{\text{sh,in}} + f_{\text{surv,stripped}} N_{\text{sh,stripped}}). \quad (3.9)$$

To bracket the (currently uncertain) resilience of cusps associated with sub ^{n} -subhalos that are released when their parent branch is tidally stripped, we explore representative choices for this parameter. The case $f_{\text{surv,stripped}} = 0$ corresponds to the most conservative limit, where cusps tied to substructure in the stripped region are assumed to be fully destroyed or efficiently mixed into the smooth host component. On the other hand, $f_{\text{surv,stripped}} = 1$ is the maximally optimistic limit in which cusps survive stripping essentially unscathed, so that all cusp contributions are retained regardless of whether their parent subhalos remain bound.

4 Results

We now quantify the annihilation enhancement from hierarchical substructure and prompt cusps in terms of the luminosity parameter,

$$J \equiv \int d^3\mathbf{x} \rho^2(\mathbf{x}), \quad (4.1)$$

which directly sets the annihilation rate for a fixed particle-physics model. The total contribution from prompt cusps can be written as

$$J_{\text{cusp, total}} = N_{\text{cusp}}(f_{\text{cusp}}, f_{\text{surv,stripped}}) \langle J_{\text{cusp}} \rangle, \quad (4.2)$$

where $\langle J_{\text{cusp}} \rangle$ is the mean cusp luminosity defined in Eq. (2.15), and $N_{\text{cusp}}(f_{\text{cusp}}, f_{\text{surv,stripped}})$ is given by Eq. (3.9).

We express the overall annihilation boost factor as an additive decomposition,

$$B = B_{\text{sh}} + B_{\text{cusp}}, \quad (4.3)$$

with each component defined by the ratio of the total substructure or cusp luminosity to that of the smooth host halo,

$$B_{\text{sh}} \equiv \frac{J_{\text{sh, total}}}{J_{\text{host}}}, \quad B_{\text{cusp}} \equiv \frac{J_{\text{cusp, total}}}{J_{\text{host}}}. \quad (4.4)$$

For the host, we adopt an NFW density profile characterized by $(\rho_{s,\text{host}}, r_{s,\text{host}})$ and concentration $c_{200,\text{host}} \equiv r_{200,\text{host}}/r_{s,\text{host}}$. The corresponding host luminosity parameter is

$$J_{\text{host}} = \int_0^{r_{200}} dr 4\pi r^2 \rho_{\text{host}}^2(r) = \frac{4\pi}{3} \rho_{s,\text{host}}^2 r_{s,\text{host}}^3 \left[1 - \frac{1}{(1 + c_{200,\text{host}})^3} \right]. \quad (4.5)$$

The total subhalo contribution $J_{\text{sh, total}}$ is computed as the weighted sum over the SASHIMI catalog [cf. Eq. (3.3)] including the contribution by up to sub ^{n} -subhalos, while the cusp component is obtained from N_{cusp} and $\langle J_{\text{cusp}} \rangle$ as above.

Figure 1 shows the mass-normalized luminosity parameters that enter the boost-factor calculation, plotted as functions of the host mass at $z = 0$. The host contribution $J_{\text{host}}/M_{\text{host}}$ decreases with increasing M_{host} , reflecting the systematic reduction in halo concentration (and hence in ρ^2 -weighted mass) toward higher masses. The subhalo contribution $J_{\text{sh, total}}/M_{\text{host}}$ varies more gently with M , as it represents an integral over the subhalo population whose internal structure and abundance evolve only mildly across the mass range considered. In contrast, the prompt-cusp contribution $J_{\text{cusp, total}}/M_{\text{host}}$ remains comparatively large over a broad range of host masses for our fiducial parameters ($f_{\text{cusp}} = 0.25$, $f_{\text{surv,stripped}} = 1$),

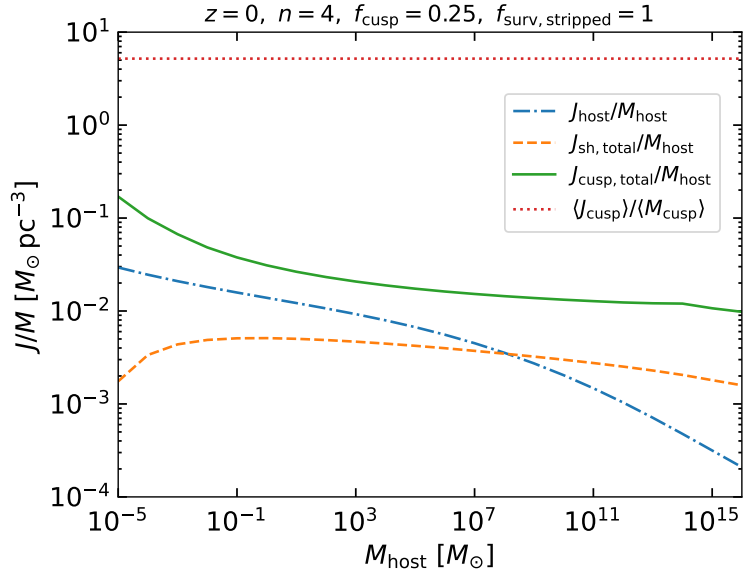


Figure 1. Mass-normalized annihilation luminosity parameters at $z = 0$ including hierarchical substructure up to sub⁴-subhalos, shown as functions of the host-halo mass M_{host} . The dot-dashed, dashed, and solid curves show the contributions from the smooth host-halo component, the total subhalo population, and the total prompt-cusp population, respectively (i.e., $J_{\text{host}}/M_{\text{host}}$, $J_{\text{sh},\text{total}}/M_{\text{host}}$, and $J_{\text{cusp},\text{total}}/M_{\text{host}}$), for the fiducial choice of $f_{\text{cusp}} = 0.25$ and $f_{\text{surv},\text{stripped}} = 1$. The dotted curve shows the intrinsic cusp annihilation efficiency, $\langle J_{\text{cusp}} \rangle / \langle M_{\text{cusp}} \rangle$.

illustrating that even a moderate surviving cusp fraction can yield a sizeable contribution to the total annihilation budget.

For comparison, we also show $\langle J_{\text{cusp}} \rangle / \langle M_{\text{cusp}} \rangle$ —the mean cusp luminosity per unit cusp mass, which is host-mass independent and is primarily controlled by the cusp internal structure and the underlying microphysical inputs. We note that $\langle J_{\text{cusp}} \rangle / \langle M_{\text{cusp}} \rangle$ corresponds to the limiting case in which the annihilation luminosity is entirely generated by cusp-like material, i.e. as if all dark matter were converted into cusps with the same internal structure. It therefore provides a useful absolute reference scale and can be viewed as an upper-envelope benchmark for the $J_{\text{cusp},\text{total}}/M_{\text{host}}$ curve, which is necessarily suppressed by the fact that only a fraction of the host mass is bound into surviving cusps in the hierarchical assembly.

Figure 2 summarizes our main result for the annihilation boost factor at $z = 0$ when hierarchical substructure is included up to sub⁴-subhalos. The colored bands visualize two independent modeling ingredients for prompt cusps. First, the overall vertical placement of each band is controlled by the cusp-occupation fraction f_{cusp} , i.e., the fraction of (sub)halos that host a surviving cusp. Second, the band width captures the additional uncertainty associated with cusps that originate from subhalos located outside the tidal truncation radius and are subsequently stripped: we bracket this effect by varying $f_{\text{surv},\text{stripped}} \in [0, 1]$, where $f_{\text{surv},\text{stripped}} = 0$ assumes complete destruction of stripped-region cusps, while $f_{\text{surv},\text{stripped}} = 1$ assumes they survive and continue to contribute. For comparison, the dotted curve shows the standard subhalo-only prediction without prompt cusps, illustrating that prompt cusps can enhance the boost but remain modest for fiducial parameter choices.

Figure 3 illustrates how the predicted boost changes as progressively deeper levels of hierarchical substructure are included. The sequence from $n = 0$ to $n = 4$ shows that the

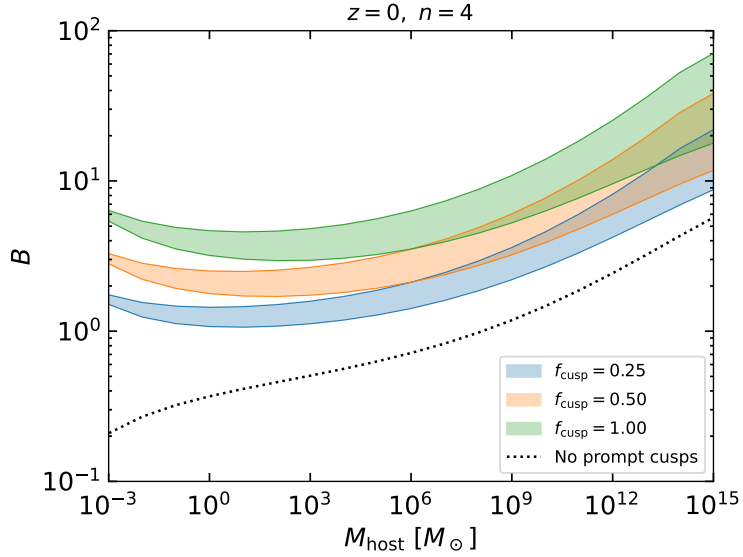


Figure 2. Annihilation boost factor $B = B_{\text{sh}} + B_{\text{cusp}}$ at $z = 0$ including hierarchical substructure up to sub⁴-subhalos, shown as a function of the host-halo mass M_{host} . The colored bands correspond to different choices of the cusp-occupation fraction f_{cusp} (0.25, 0.5, and 1 from bottom to top). For each f_{cusp} , the band width reflects uncertainty in the survival of cusps associated with the stripped region, parametrized by $f_{\text{surv,stripped}} \in [0, 1]$: the lower (upper) edge assumes $f_{\text{surv,stripped}} = 0$ (1). The dotted curve shows the baseline prediction without prompt cusps ($B = B_{\text{sh}}$).

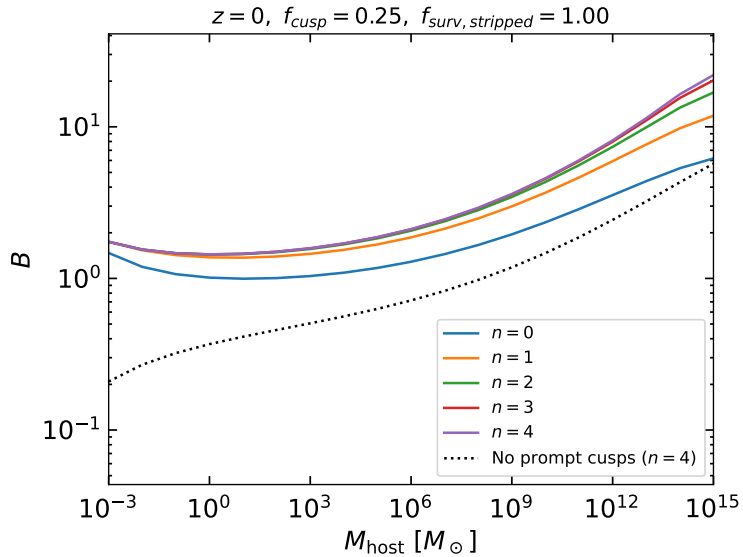


Figure 3. Dependence of the total boost factor B on the depth of hierarchical substructure included in the model. Curves show results at $z = 0$ for $n = 0, \dots, 4$ (from bottom to top), where n denotes inclusion up to sub ^{n} -subhalos. The dotted curve shows the corresponding reference prediction without prompt cusps (for $n = 4$).

hierarchy rapidly approaches a converged result once a few substructure levels are accounted for; i.e. the incremental impact of adding ever higher-order sub-substructure becomes small.

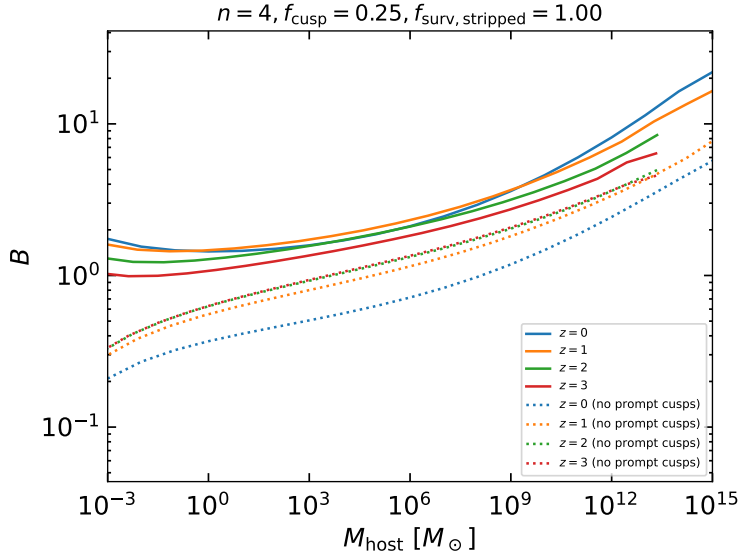


Figure 4. Redshift dependence of the total boost factor B as a function of host-halo mass M_{host} . Solid curves include prompt cusps, while dotted curves show the corresponding no-cusp baseline, for $z = 0, 1, 2$, and 3 (from top to bottom at high masses).

For comparison, the dotted curve shows the no-cusp baseline evaluated at $n = 4$.

Figure 4 shows the redshift evolution of the boost factor. At fixed host mass, the boost varies with z due to the changing halo structural properties and the shorter time available for hierarchical buildup and tidal processing at earlier epochs. In all cases, the prompt-cusp contribution (solid) shifts the boost above the no-cusp baseline (dotted), while preserving the overall mass trend. This figure therefore provides a compact summary of how both the subhalo hierarchy and prompt cusps jointly shape $B(M_{\text{host}}, z)$.

5 Discussion

5.1 Comparison with earlier work

For similar benchmark assumptions as in the universal-average treatment of Ref. [26] ($f_{\text{cusp}} = 0.25$ and $f_{\text{surv,stripped}} = 1$), our predicted Milky-Way-size boost is $B \sim \mathcal{O}(10)$ at $z = 0$, about one order of magnitude smaller than the ~ 100 quoted by Delos and White [26]. This offset can be understood primarily as a difference in the inferred abundance of surviving cusps: their Fig. 4 suggests $N_{\text{cusp}} \sim 4 \times 10^{16}$ in a $10^{12} M_{\odot}$ halo, whereas Table 1 combined with Eq. (3.9) yields $N_{\text{cusp}} \sim 3 \times 10^{15}$. Since $J_{\text{cusp},\text{total}} \propto N_{\text{cusp}} \langle J_{\text{cusp}} \rangle$ at fixed cusp internal structure, a one-dex difference in N_{cusp} maps directly onto a one-dex difference in B . Equivalently, adopting the typical prompt-cusp mass $\langle M_{\text{cusp}} \rangle \sim 10^{-6} M_{\odot}$ (Eq. 2.15 and surrounding discussion), the implied total mass bound in cusps is $M_{\text{cusp},\text{tot}} \sim N_{\text{cusp}} \langle M_{\text{cusp}} \rangle \sim 4 \times 10^{10} M_{\odot}$ in the Delos and White estimate (i.e. $\sim 4\%$ of a $10^{12} M_{\odot}$ host), while our hierarchical SASHIMI-based count implies $M_{\text{cusp},\text{tot}} \sim 3 \times 10^9 M_{\odot}$ (i.e. $\sim 0.3\%$ of the host mass).

5.2 Possible origin of the cusp-abundance difference

At present, the origin of the cusp-count mismatch can only be discussed qualitatively, and a quantitative reconciliation is beyond the scope of this work. Nevertheless, several differences

in modeling philosophy plausibly contribute.

First, our cusp abundance inherits the EPS-based merger-tree construction underlying SASHIMI, whereas Ref. [26] builds cusp statistics from peak theory using a universal-average mapping. EPS prescriptions are often calibrated primarily on relatively massive haloes, so their extrapolation into the microhalo regime is not guaranteed *a priori*. On the other hand, recent ultra-high-resolution simulations of void environments find that EPS, treated as a conditional mass function, can remain accurate down to $M \sim 10^{-6} M_\odot$ in underdense regions [41]. This supports the plausibility of EPS-based extrapolations in at least some environments, while leaving open the possibility that peak-selection effects or environmental conditioning can generate larger deviations in massive hosts.

Second, Ref. [26] effectively counts cusps associated with peaks that collapse down to $z = 0$. In contrast, our implementation assigns cusps at the formation of (sub)halos within the hierarchical tree and does not create additional cusps within an already-accreted branch; subsequent evolution can only reduce the identifiable cusp population through stripping or disruption. If late-time cusp formation in already-accreted material is non-negligible, our procedure will undercount cusps relative to a universal peak-based estimate.

Third, microhalo-scale structures that host primordial cusps are expected to be weakly clustered ($b < 1$) relative to dark matter particles in many environments, whereas a universal-average mapping effectively assumes an unbiased distribution when translating “cusps per unit mass” into “cusps per host” independent of environment. Even a modest anti-bias could reduce the expected cusp abundance in Milky-Way-like regions relative to the universal estimate.

Lastly, an additional, and potentially important, source of uncertainty in the EPS-based microhalo abundance concerns the mapping between the cutoff scale and halo mass when computing $\sigma(M)$ for a suppressed small-scale power spectrum. In SASHIMI we evaluate $\sigma(M)$ with a sharp- k filter and adopt a cutoff $k_{\max} = \alpha/R$, where α parametrizes the residual ambiguity of this mapping [38]. Our fiducial choice, $\alpha = 1.8$, is motivated by matching to the real-space top-hat result in the large-mass regime, but it is not calibrated directly on microhalo simulations. Crucially, varying α can change the predicted abundance of microhaloes—and hence the inferred number of prompt cusps—without dramatically affecting the mass function on the high-mass end that dominates typical calibrations. For example, we find that choosing $\alpha = 1$ increases the predicted cusp abundance by a factor of ~ 5 relative to the fiducial model, while $\alpha = 2.5$ reduces it to ~ 0.4 times the fiducial value. This sensitivity suggests that a dedicated calibration of α in the microhalo regime (e.g. using ultra-high-resolution simulations that resolve Earth-mass haloes and their environmental dependence) will be important for robust predictions of N_{cusp} and, in turn, of the cusp-induced annihilation boost.

5.3 Future directions

A definitive resolution of the order-of-magnitude difference to universal-average predictions likely requires a unified framework that embeds peak-based cusp formation criteria into merger-tree evolution with explicit environmental conditioning. There is relevant groundwork connecting peaks and excursion-set ideas, such as excursion-set peaks and related peak-constrained excursion-set formalisms [42, 43]. Complementary peak-based methods that generate halo catalogs and assembly histories directly from the initial density field—e.g. peak-patch [39] and PINOCCHIO [44, 45]—may also provide useful routes for marrying cusp-scale peak properties to hierarchical growth. Adapting such approaches to prompt cusps (including

the mapping from peak parameters to cusp structural parameters and survival probabilities) is an interesting direction for future work.

6 Conclusions

Recent simulations indicate that the earliest collapsing peaks in the primordial density field can form steep “prompt cusps” with $\rho \propto r^{-3/2}$ and that a substantial fraction may survive hierarchical growth to $z = 0$ in WIMP-like CDM scenarios [24–26]. Motivated by these developments, we implemented prompt cusps in the semi-analytic substructure framework SASHIMI [17, 18], enabling a hierarchical and environment-dependent treatment of annihilation enhancement beyond the universal-average boost approach. We summarize our main findings as follows:

- The predicted contribution from hierarchical substructure converges rapidly with the depth of the hierarchy: including up to sub³–sub⁴-subhalos is sufficient for a stable boost prediction in the mass range studied (Fig. 3).
- Prompt cusps provide an additional component to the annihilation luminosity that can raise the total boost above the standard subhalo-only expectation. For fiducial survival assumptions ($f_{\text{cusp}} = 0.25$ and $f_{\text{surv,stripped}} = 1$), we find $B \sim \mathcal{O}(10)$ for Milky-Way-like hosts at $z = 0$ (Fig. 2), while the no-cusp baseline remains at $B_{\text{sh}} \sim \text{few}$.
- Across host masses and redshifts, prompt cusps increase the normalization of $B(M_{\text{host}}, z)$ while largely preserving the qualitative mass and redshift trends of the baseline prediction (Fig. 4). The dominant theoretical uncertainty is captured by the cusp-occupation fraction f_{cusp} and the survival of cusps associated with stripped material, $f_{\text{surv,stripped}}$.

Compared to the universal-average peak-based estimate of Delos and White [26], our fiducial Milky-Way boost is lower by about one order of magnitude, which we attribute primarily to a correspondingly lower inferred number of cusps in a host. This difference highlights the importance of unifying peak-based cusp formation statistics with merger-tree evolution and environmental conditioning. Our SASHIMI-based implementation provides a flexible platform for pursuing this goal and for propagating improved cusp-formation and survival prescriptions into testable predictions for annihilation signals.

Acknowledgments

This work was partly supported by MEXT KAKENHI Grant Numbers, JP20H05850, JP20H05861, and JP24K07039.

References

- [1] S. Hofmann, D.J. Schwarz and H. Stöcker, *Damping scales of neutralino cold dark matter*, *Physical Review D* **64** (2001) .
- [2] S. Profumo, K. Sigurdson and M. Kamionkowski, *What mass are the smallest protohalos?*, *Phys. Rev. Lett.* **97** (2006) 031301.
- [3] E. Bertschinger, *The Effects of Cold Dark Matter Decoupling and Pair Annihilation on Cosmological Perturbations*, *Phys. Rev. D* **74** (2006) 063509 [[astro-ph/0607319](#)].

[4] A.M. Green, S. Hofmann and D.J. Schwarz, *The power spectrum of susy-cdm on subgalactic scales: Cdm power spectrum on subgalactic scales*, *Monthly Notices of the Royal Astronomical Society* **353** (2004) L23–L27.

[5] A. Loeb and M. Zaldarriaga, *The Small-scale power spectrum of cold dark matter*, *Phys. Rev. D* **71** (2005) 103520 [[astro-ph/0504112](#)].

[6] R. Diamanti, M.E.C. Catalan and S. Ando, *Dark matter protohalos in a nine parameter MSSM and implications for direct and indirect detection*, *Phys. Rev. D* **92** (2015) 065029 [[1506.01529](#)].

[7] J. Silk and A. Stebbins, *Clumpy cold dark matter*, *Astrophys. J.* **411** (1993) 439.

[8] L. Bergstrom, J. Edsjo, P. Gondolo and P. Ullio, *Clumpy neutralino dark matter*, *Phys. Rev. D* **59** (1999) 043506 [[astro-ph/9806072](#)].

[9] L. Bergstrom, J. Edsjo and P. Ullio, *Possible indications of a clumpy dark matter halo*, *Phys. Rev. D* **58** (1998) 083507 [[astro-ph/9804050](#)].

[10] S. Ando, *Can dark matter annihilation dominate the extragalactic gamma-ray background?*, *Phys. Rev. Lett.* **94** (2005) 171303 [[astro-ph/0503006](#)].

[11] L. Pieri, G. Bertone and E. Branchini, *Dark Matter Annihilation in Substructures Revised*, *Mon. Not. Roy. Astron. Soc.* **384** (2008) 1627 [[0706.2101](#)].

[12] S.M. Koushiappas, A.R. Zentner and T.P. Walker, *The observability of gamma-rays from neutralino annihilations in Milky Way substructure*, *Phys. Rev. D* **69** (2004) 043501 [[astro-ph/0309464](#)].

[13] F. Stoehr, S.D.M. White, V. Springel, G. Tormen and N. Yoshida, *Dark matter annihilation in the halo of the Milky Way*, *Mon. Not. Roy. Astron. Soc.* **345** (2003) 1313 [[astro-ph/0307026](#)].

[14] V. Berezinsky, V. Dokuchaev and Y. Eroshenko, *Anisotropy of dark matter annihilation with respect to the Galactic plane*, *JCAP* **07** (2007) 011 [[astro-ph/0612733](#)].

[15] J. Lavalle, Q. Yuan, D. Maurin and X.J. Bi, *Full Calculation of Clumpiness Boost factors for Antimatter Cosmic Rays in the light of Lambda-CDM N-body simulation results. Abandoning hope in clumpiness enhancement?*, *Astron. Astrophys.* **479** (2008) 427 [[0709.3634](#)].

[16] R. Bartels and S. Ando, *Boosting the annihilation boost: Tidal effects on dark matter subhalos and consistent luminosity modeling*, *Phys. Rev. D* **92** (2015) 123508 [[1507.08656](#)].

[17] N. Hiroshima, S. Ando and T. Ishiyama, *Modeling evolution of dark matter substructure and annihilation boost*, *Phys. Rev. D* **97** (2018) 123002 [[1803.07691](#)].

[18] S. Ando, T. Ishiyama and N. Hiroshima, *Halo substructure boosts to the signatures of dark matter annihilation*, *Galaxies* **7** (2019) 68.

[19] T. Ishiyama and S. Ando, *The Abundance and Structure of Subhaloes near the Free Streaming Scale and Their Impact on Indirect Dark Matter Searches*, *Mon. Not. Roy. Astron. Soc.* **492** (2020) 3662 [[1907.03642](#)].

[20] J.F. Navarro, C.S. Frenk and S.D.M. White, *A universal density profile from hierarchical clustering*, *The Astrophysical Journal* **490** (1997) 493.

[21] T. Ishiyama, J. Makino and T. Ebisuzaki, *Gamma-ray Signal from Earth-mass Dark Matter Microhalos*, *Astrophys. J. Lett.* **723** (2010) L195 [[1006.3392](#)].

[22] D. Anderhalden and J. Diemand, *Density Profiles of CDM Microhalos and their Implications for Annihilation Boost Factors*, *JCAP* **04** (2013) 009 [[1302.0003](#)].

[23] T. Ishiyama, *Hierarchical Formation of Dark Matter Halos and the Free Streaming Scale*, *Astrophys. J.* **788** (2014) 27 [[1404.1650](#)].

[24] M.S. Delos and S.D.M. White, *Inner cusps of the first dark matter haloes: formation and survival in a cosmological context*, *Monthly Notices of the Royal Astronomical Society* **518**

(2022) 3509
[\[https://academic.oup.com/mnras/article-pdf/518/3/3509/47466116/stac3373.pdf\]](https://academic.oup.com/mnras/article-pdf/518/3/3509/47466116/stac3373.pdf).

[25] M.S. Delos, M. Korsmeier, A. Widmark, C. Blanco, T. Linden and S.D.M. White, *Limits on dark matter annihilation in prompt cusps from the isotropic gamma-ray background*, 2024.

[26] M.S. Delos and S.D.M. White, *Prompt cusps and the dark matter annihilation signal*, *JCAP* **10** (2023) 008 [[2209.11237](#)].

[27] J. Stücker, G. Ogiya, S.D.M. White and R.E. Angulo, *The effect of stellar encounters on the dark matter annihilation signal from prompt cusps*, *Mon. Not. Roy. Astron. Soc.* **523** (2023) 1067 [[2301.04670](#)].

[28] M. Crnogorčević, M.S. Delos, N. Kuritzén and T. Linden, *Gamma-ray observations of galaxy clusters strongly constrain dark matter annihilation in prompt cusps*, *Phys. Rev. D* **112** (2025) 103001 [[2501.14865](#)].

[29] A. Dekker, S. Ando, C.A. Correa and K.C.Y. Ng, *Warm dark matter constraints using Milky Way satellite observations and subhalo evolution modeling*, *Phys. Rev. D* **106** (2022) 123026 [[2111.13137](#)].

[30] S. Ando, S. Horigome, E.O. Nadler, D. Yang and H.-B. Yu, *SASHIMI-SIDM: semi-analytical subhalo modelling for self-interacting dark matter at sub-galactic scales*, *JCAP* **02** (2025) 053 [[2403.16633](#)].

[31] M.S. Delos, M. Bruff and A.L. Erickcek, *Predicting the density profiles of the first halos*, *Phys. Rev. D* **100** (2019) 023523.

[32] Planck Collaboration, Aghanim, N., Akrami, Y., Ashdown, M., Aumont, J., Baccigalupi, C. et al., *Planck 2018 results - vi. cosmological parameters*, *Astron. Astrophys.* **641** (2020) A6.

[33] J.M. Bardeen, J.R. Bond, N. Kaiser and A.S. Szalay, *The Statistics of Peaks of Gaussian Random Fields*, *Astrophys. J.* **304** (1986) 15.

[34] D.J. Eisenstein and W. Hu, *Baryonic features in the matter transfer function*, *Astrophys. J.* **496** (1998) 605 [[astro-ph/9709112](#)].

[35] A.M. Green, S. Hofmann and D.J. Schwarz, *The power spectrum of SUSY - CDM on sub-galactic scales*, *Mon. Not. Roy. Astron. Soc.* **353** (2004) L23 [[astro-ph/0309621](#)].

[36] R.K. Sheth, H.J. Mo and G. Tormen, *Ellipsoidal collapse and an improved model for the number and spatial distribution of dark matter haloes*, *Mon. Not. Roy. Astron. Soc.* **323** (2001) 1 [[astro-ph/9907024](#)].

[37] S. Tremaine and J.E. Gunn, *Dynamical Role of Light Neutral Leptons in Cosmology*, *Phys. Rev. Lett.* **42** (1979) 407.

[38] A. Schneider, R.E. Smith and D. Reed, *Halo Mass Function and the Free Streaming Scale*, *Mon. Not. Roy. Astron. Soc.* **433** (2013) 1573 [[1303.0839](#)].

[39] J.R. Bond and S.T. Myers, *The Hierarchical peak patch picture of cosmic catalogs. 1. Algorithms*, *Astrophys. J. Suppl.* **103** (1996) 1.

[40] J.R. Bond and S.T. Myers, *The Hierarchical peak patch picture of cosmic catalogs. 2. Validation and application to clusters*, *Astrophys. J. Suppl.* **103** (1996) 41.

[41] H. Zheng, S. Bose, C.S. Frenk, L. Gao, A. Jenkins, S. Liao et al., *The abundance of dark matter haloes down to Earth mass*, *Mon. Not. Roy. Astron. Soc.* **528** (2024) 7300 [[2310.16093](#)].

[42] A. Paranjape and R.K. Sheth, *Peaks theory and the excursion set approach*, *Mon. Not. Roy. Astron. Soc.* **426** (2012) 2789 [[1206.3506](#)].

[43] A. Paranjape, R.K. Sheth and V. Desjacques, *Excursion set peaks: a self-consistent model of dark halo abundances and clustering*, *Mon. Not. Roy. Astron. Soc.* **431** (2013) 1503 [[1210.1483](#)].

- [44] P. Monaco, T. Theuns and G. Taffoni, *Pinocchio: pinpointing orbit-crossing collapsed hierarchical objects in a linear density field*, *Mon. Not. Roy. Astron. Soc.* **331** (2002) 587 [[astro-ph/0109323](#)].
- [45] G. Taffoni, P. Monaco and T. Theuns, *Pinocchio and the hierarchical build-up of dark matter haloes*, *Mon. Not. Roy. Astron. Soc.* **333** (2002) 623 [[astro-ph/0109324](#)].